Contribution from the Department of Chemistry,
Stanford University, Stanford, California 94305

Reactivity of Imidazoliumruthenium Ammine Complexes: Nitrogen- to Carbon-Bound Rearrangement, Trans Labilization, and Redox Behavior

M. F. TWEEDLE and H. TAUBE*

Received October 29, 1981

In *trans*-$H_2O(NH_3)_4Ru^{III}L$, where L is carbon-bound[4,5] dimethylimidazole, the affinity for imidazole, pyridine, isonicotinamide, Cl^-, Br^-, or I^- is reduced to such a degree that K_{assoc} could not be measured directly and the upper limit on K_{assoc} is ca. 5. For isonicotinamide, it was calculated as 1.2 from the relevant redox potentials and the measured value of K_{assoc} for the Ru(II) form of the complex. The reaction with NCS^- is rather rapid, and this points to a large kinetic labilization produced in Ru(III) by the C-bound ligand replacing NH_3. In this case, the affinity remains high—$K_{assoc} = 3.3 \times 10^4$. The value of pK_a governing the deprotonation of H_2O trans to C-bound imidazole on Ru(III) is 6.9; that governing the deprotonation of the C-bound imidazole itself in the pentaammine complex is 11.0. The rate of isomerization of N-bound imidazole to the C-bound form on Ru(II) was studied as a function of acidity. In each case, isomerization is accompanied by aquation, and each reaction is first order in $[H^+]$. The percent yields of the C-bound products are 0, 5, 20, and 85 for 1-methylimidazole, imidazole, 4,5-dimethylimidazole, and histidine, respectively. Rearrangement is an intramolecular process. The oxidation by H_2O_2 of *trans*-$H_2O(NH_3)_4Ru^{II}L$ (where L is C-bound 4,5-dimethylimidazole) to the Ru(III) product is complicated by destruction of the ligand and by decomposition of H_2O_2. The specific rate governing the disappearance of Ru(II) is 1.9×10^3 M^{-1} s^{-1}, and we infer that it involves substitution on the metal center. An inner-sphere mode also obtains in the oxidation with O_2. The specific rate governing the disappearance of Ru(II) where L now is C-bound imidazole is 1.36×10^2 M^{-1} s^{-1}. All the data cited in the foregoing were obtained at 25 °C.

Introduction

Imidazole and its derivatives, particularly histidine and benzimidazole, are of interest as ligands owing to their prominent role in the biological chemistry of transition-metal ions.[1] Most transition metals have been shown to complex imidazole, in the majority of cases through the lone pair on nitrogen 3.[1] In striking exception to this behavior are certain complexes of ruthenium ammines in which the ligand is bound to ruthenium at carbon 2 of the ring.[2] The ligand bound in this mode is formally the imidazolium ylide, a neutral, dipolar tautomer of imidazole possessing an unshared pair of σ electrons on carbon 2:

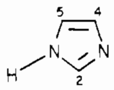

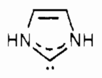

Sundberg et al.[2,3] first prepared and characterized a number of C-bound imidazole complexes of ruthenium. Several additional derivatives have been prepared since,[4-6] but their chemistry has not been investigated thoroughly. The work described herein was undertaken to explore basic aspects of the reactivity of the title complexes in aqueous solution. It includes the study of their acid-catalyzed formation, substitution reactions, electrochemical behavior, and reactions with hydrogen peroxide and oxygen.

Abbreviations used in this paper are as follows: BzIm ≡ benzimidazole; Me_2Im ≡ 4,5-dimethylimidazole; Hist ≡ histidine; Im ≡ imidazole; isn ≡ isonicotinamide; $Mepyr^+$ ≡ *N*-methylpyrazinium ion; *N*-MeIm ≡ 1-methylimidazole; $TFMS^-$ ≡ trifluoromethanesulfonate ion; NCpy ≡ 4-cyanopyridine; py ≡ pyridine; pz ≡ pyrazine; obsd ≡ observed.

The mode of binding to the metal will be indicated by a suffix C or N. It is understood, unless otherwise indicated, that C-bound species are *trans*-tetraammine aquo species, and N-bound species are pentaammines. Thus $Ru(Im\text{-}C)^{2+}$ represents *trans*-tetraammineaquo(2-imidazolium)ruthenium(II); $Ru(Im\text{-}N)^{2+}$ represents pentaammineimidazoleruthenium(II). Note that the imidazolium moiety is a neutral species.

Experimental Section

Materials. House deionized water was distilled from alkaline permanganate. Standard HCl, NaOH, and $Na_2S_2O_3$ were prepared by diluting E. Merck Titrisol ampules. Trifluoromethanesulfonic acid from 3M Co. (300 mL) was doubly vacuum distilled and the distillate diluted to 600 mL. For the removal of turbidity that appeared on dilution, 30–40 mL of the diluted acid was distilled off and discarded, leaving a transparent solution.[7] The salt NaTFMS was precipitated by neutralizing a freshly distilled HTFMS solution (~18 N) with Na_2CO_3, recrystallized from hot water and dried at 120 °C to a constant weight.

Imidazole (Aldrich) was recrystallized from benzene. Dimethylimidazole was prepared by a published method[8] and recrystallized from boiling chloroform before use. It is oxygen sensitive in chloroform, but the solid decomposes only slowly (weeks) in a vacuum desiccator. Other imidazoles, BzIm (Aldrich), *N*-MeIm (Aldrich), and Hist (Matheson), were used as received.

Isonicotinamide (Aldrich) was recrystallized from hot water. Methylpyrazinium iodide and $TFMS^-$ salts were prepared by the method of Magnuson.[9] Sodium thiocyanate was recrystallized from ethanol and dried in a vacuum desiccator.

Ion exchange was performed on glass columns with purified[10] Bio-Rad Ag50W-X2 200–400-mesh cation resin in the proton form. Similar results were obtained in several cases from SP-Sephadex C-25 resin.

Ruthenium Solutions. Solutions of Ru(III) were prepared by dissolving the trichloride salts in water. When *trans*-$[(NH_3)_4Ru(2\text{-imidazolium})Cl]Cl_2$ is dissolved, the coordinated chloride is readily replaced by water. Chloride was removed with use of a stoichiometric amount of AgO_2CCF_3. The concentration of ruthenium was determined spectrophotometrically after reduction as described in the next paragraph, analysis in the 2+ state being preferred because the charge-transfer bands of the Ru(III) species are more medium sensitive.

The Ru(II) species are readily oxidized by air. They were generated in situ by first deoxygenating the parent Ru(III) solution with argon that had been scrubbed by a solution of Cr(II) and then reducing with Zn amalgam under argon.

Preparations. With the single exception described in detail below, the Ru(III) complexes (as chloride salts) were prepared by following published procedures.[3,6] The analytical results for all are summarized in Chart I.

---

(1) Sundberg, R. J.; Martin, R. B. *Chem. Rev.* **1974**, *74*, 471.
(2) Sundberg, R. J.; Shepherd, R. E.; Taube, H. *J. Am. Chem. Soc.* **1972**, *94*, 6558.
(3) Sundberg, R. J.; Bryan, R. F.; Taylor, I. F., Jr.; Taube, H. *J. Am. Chem. Soc.* **1974**, *96*, 381.
(4) Krentzien, H. J.; Clarke, M. J.; Taube, H. *Bioinorg. Chem.* **1975**, *4*, 143.
(5) Clarke, M. J.; Taube, H. *J. Am. Chem. Soc.* **1975**, *97*, 1397.
(6) Sundberg, R. J.; Gupta, G. *Bioinorg. Chem.* **1973**, *3*, 39.
(7) Willis, M. Ph.D. Thesis, Stanford University, 1976.
(8) Bredereck, H.; Theilig, G. *Chem. Ber.* **1953**, *86*, 88.
(9) Magnuson, R. H. Ph.D. Thesis, Stanford University, 1973.
(10) Deutsch, E. A. Ph.D. Thesis, Stanford University, 1967.

0020-1669/82/1321-3361$01.25/0

Chart I. Analytical Data

		%C	%H	%N
$[(NH_3)_5Ru(Im\text{-}\mathit{N})]Cl_3\cdot 0.5CH_3CH_2OH$	calcd	12.52	6.57	25.55
	found	12.45	6.21	25.15
$[(NH_3)_5Ru(Me_2Im\text{-}\mathit{N})]Cl_3\cdot 3H_2O$	calcd	13.56	6.60	22.14
	found	13.80	6.10	21.75
$[(NH_3)_5Ru(Hist\text{-}\mathit{N})]Cl_3\cdot 1.5H_2O$	calcd	15.18	5.73	23.60
	found	15.42	5.45	23.38
$[(NH_3)_5Ru(BzIm\text{-}\mathit{N})]Cl_3\cdot 2H_2O$	calcd	18.82	5.64	21.95
	found	18.57	5.03	21.12
trans-$[(NH_3)_4ClRu(Im\text{-}\mathit{C})]Cl_2$	calcd	10.48	4.69	24.46
	found	10.33	4.59	24.57
trans-$[(NH_3)_4ClRu(Me_2Im\text{-}\mathit{C})]Cl_2\cdot 0.5\ H_2O$	calcd	15.77	5.56	22.07
	found	15.66	5.29	22.18
trans-$[(NH_3)_4ClRu(BzIm\text{-}\mathit{C})]Cl\cdot H_2O$	calcd	20.42	4.90	20.41
	found	20.42	4.53	20.08
$[(NH_3)_3Cl_2Ru(Me_2Im\text{-}\mathit{C})]Cl$	calcd	16.93	4.83	19.75
	found	16.89	5.04	19.39

Not hitherto described is the preparation of triammine(4,5-dimethyl-2-imidazolium)ruthenium(III) trichloride. For its preparation, a solution of $Ru(Me_2Im\text{-}\mathit{C})^{3+}$ (30 mg of the trichloride in 10 mL of 0.1 M KCl at pH 4) was oxidized at a Pt-basket electrode at a controlled potential of +0.94 V vs. SCE for 15 min. The solution was loaded on an ion-exchange column and eluted with HCl. A fraction eluted with 1.0 M HCl showed a band in the UV at 335 nm. A solution of 2 M HCl eluted an unidentified product that absorbed at 540 nm and 335 nm, while 2.5–3 M HCl eluted a product that absorbed at 598 and 335 nm, followed by some residual $Ru(Me_2Im\text{-}\mathit{C})^{3+}$. The 2.5–3.0 M HCl fraction was stripped to dryness on a rotary evaporator. The light purple solid residue was dissolved in a minimum quantity of water and precipitated with acetone. The solid formed was isolated by centrifugation, washed with acetone, and dried in a vacuum desiccator. The product showed absorption bands at 598 (ϵ = 3700) and 335 nm (ϵ = 3500) in 0.10 N HCl. These two bands were also observed in a preparation of $Ru(Me_2Im\text{-}\mathit{C})^{3+}$, when a reaction between $Me_2Im\text{–}Me_2ImH^+$ (0.12 M) and $(NH_3)_5RuH_2O^{2+}$ (0.02 M) at pH 5 was allowed to proceed for 16 h rather than 8–10 h as specified in ref 3.

Standardization. Hydrogen peroxide (J. T. Baker 3% or 30%) was standardized by iodometric methods, with Mo(VI) as a catalyst for the reaction of H_2O_2 with I^-.

Oxygen-saturated solutions were prepared by bubbling oxygen (Liquid Carbonic) through a solution for 1 h. Prebubblers were used for volatile acidic solutions. Four oxygen-saturated 0.10 N HTFMS solutions were analyzed for oxygen[11] and found to be $(1.2 \pm 0.05) \times 10^{-3}$ M. The oxyygen concentration at saturation was thereafter assumed to be 1.2×10^{-3} M. Gastight syringes fitted with low-volume 26-gauge platinum needles were used to mix oxygen-saturated and argon-saturated solutions to obtain lower concentrations of oxygen. Air-saturated solutions were assumed to be 2.5×10^{-4} M in oxygen.[12] Atmospheric pressure did not change significantly over the time needed to do a series of runs at varying O_2 concentration.

Measurements. A Beckman UV5270 or Cary 14 instrument was used for spectrophotometric measurements. pH was measured with a Brinkman Model 101 pH meter. Electrochemical potentials were measured by cyclic voltammetry on a PAR Model 173 potentiostat–Model 175 programmer system with a platinum button or a hanging-mercury-drop indicator electrode, a platinum-wire working electrode, and an SCE reference electrode. Scan rates were 100–200 mV s^{-1}. Formal potentials, E_f, were taken to be the mean of the anodic and cathodic peaks. The observed potentials were converted to the NHE scale by adding 0.244 V. Solutions were 10^{-4}–10^{-3} M in substrate and usually 0.10 N in electrolyte. $Ru(NH_3)_6Cl_3$ (E_f(3+/2+) = 0.060 V vs. NHE)[13] was used for calibration.

Kinetics. Rates were measured under pseudo-first-order conditions by standard spectrophotometric methods when $t_{1/2} > 5$ s and with an Aminco-Morrow stopped-flow apparatus for faster reactions. Stritar's[14] method was used for data reduction. For the stopped-flow work, data were taken through 3 half-lives to obtain a first-order rate constant from the slope of semilog plots by linear regression.

Table I. Substitution of $Ru(Me_2Im\text{-}\mathit{C})^{3+}$ by NCS^- at $\mu = 1.0$

$10^3 \times [NCS^-]$, M	$10^3 \times k_{obsd}$, s^{-1}	$10^{-2} \times k_{obsd}^{-1}$, s^{-1}	$10^3 \times [NCS^-]$, M	$10^3 \times k_{obsd}$, s^{-1}	$10^{-2} \times k_{obsd}^{-1}$, s^{-1}
9.7	1.4	7.2	127	12.3	0.81
15.5	2.9	3.4	327	13.5	0.74
25.4	4.8	2.1	490	15.0	0.67
70	9.6	1.04			

Quantitative transfers of air-sensitive materials were made by Hamilton gastight syringes with Pt needles. Contact of reagents with material other than glass, Teflon, polypropylene, and platinum was avoided. Ionic strength was controlled with NaTFMS except where otherwise indicated.

Results

Because the complexes in both the 3+ and the 2+ oxidation states are substitution labile in the trans position, the properties depend on the composition of the environment. For this reason, substitution dynamics will be dealt with before properties such as absorption spectra and formal potentials are summarized.

Ruthenium(III) complexes were isolated as trichloride salts. The N-bound complexes are pentaammines and, in solution, are substitution inert. The Ru(II) C-bound complexes were shown to be tetraammines in solution by their NMR spectra.[3,5,6] Molecular structure determinations by X-ray crystallography have verified the geometry of *trans*-$[(NH_3)_4Ru(Me_2Im\text{-}\mathit{C})(CO)](PF_6)_2$,[3] and only cis ammines were found in the X-ray structure of *trans*-$[(NH_3)_3Ru(caffeine\text{-}\mathit{C})Cl_2]Cl\cdot H_2O$.[4] The C-bound derivatives are therefore assumed to be trans tetraammines, and on the time scale of most of the experiments, they retain integrity at the ammine and C-bound positions. When the trichloride of $Ru(Me_2Im\text{-}\mathit{C})^{3+}$ is dissolved, coordinated chloride is readily replaced by water.[3]

Ruthenium(III) Complexes. Interaction with Halides. We attempted to measure the affinity of $Ru(Me_2Im\text{-}\mathit{C})^{3+}$ for Cl^-, Br^-, and I^- spectrophotometrically, but it was evident that at halide concentrations up to 4 M complex formation was still incomplete. The association equilibrium quotients were estimated to be less than 5 at μ = 4.0 (25 °C). For comparison, the affinity of Cl^- for $(NH_3)_5RuH_2O^{3+}$ is 1.2×10^2.[15]

Nitrogen Bases as Ligands. The affinity of $Ru(Me_2Im\text{-}\mathit{C})^{3+}$ for nitrogen heterocyclic bases, Im, py, isn, and pzH^+, could not be measured directly because it was too low. For isn, however, the affinity quotient is calculated as 1.2 from the measured affinity of isn for $Ru(Me_2Im\text{-}\mathit{C})^{2+}$, $K = 7.2 \times 10^2$, and the formal potentials of $Ru(Me_2Im\text{-}\mathit{C})^{3+/2+}$, E_f = 0.130 V, and $Ru(Me_2Im\text{-}\mathit{C})(isn)^{3+/2+}$, E_f = 0.295 V. For $(NH_3)_5RuH_2O^{3+}$ the corresponding affinity quotient is 6×10^3.[16,17]

NCS^- as Ligand. Ligation of NCS^- by $Ru(Me_2Im\text{-}\mathit{C})^{3+}$ features some unusual effects. As will be shown, the affinity quotient is high and the reaction is slow enough to make feasible measurements of rate with the spectrophotometer. The reaction was followed at 450 nm, where a shoulder on the 600-nm band grew when $Ru(Me_2Im\text{-}\mathit{C})^{3+}$ was treated with NaNCS. The kinetics were measured under pseudo-first-order conditions in excess NaNCS. The data are listed in Table I and shown plotted as k_{obsd} vs. $[NCS^-]$ in Figure 1a. A line through the points at low $[NCS^-]$ has a slope of 2.12×10^{-1} M^{-1} s^{-1} and an intercept near zero (-5.5×10^{-5} s^{-1}). At higher $[NCS^-]$ the observed rates level off sharply. So abrupt is the approach to saturation, that a second stage for labile association of $[NCS^-]$ is indicated. The simplest mechanism that

---

(11) Pladziewicz, J. R.; Meyer, T. J.; Broomhead, J. A.; Taube, H. *Inorg. Chem.* **1973**, *12*, 639.

(12) "The Merck Index"; 8th ed.; Merck and Co.: Rahway, NJ, 1968; p 109.

(13) Diamond, S. E.; Tom, G. M.; Taube, H. *J. Am. Chem. Soc.* **1975**, *97*, 2661.

(14) Stritar, J. A. Ph.D. Thesis, Stanford University, 1967.

(15) Broomhead, J. A.; Basolo, F.; Pearson, R. G. *Inorg. Chem.* **1964**, *3*, 826.

(16) Taube, H. *Coord. Chem. Rev.* **1978**, *26*, 33.

(17) Shepherd, R. E.; Taube, H. *Inorg. Chem.* **1973**, *12*, 1392.

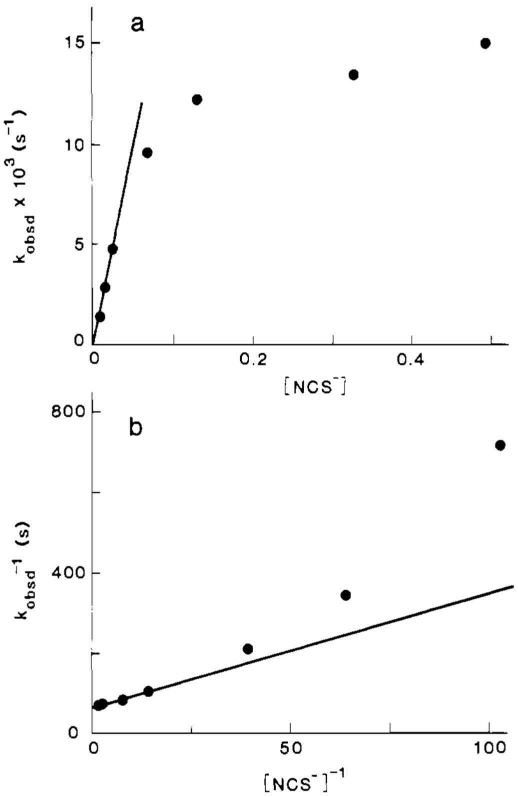

Figure 1. Kinetics of the reaction of NCS^- with $Ru(Me_2Im\text{-}C)^{3+}$ (μ = 1.0; 25.0 °C; pH 4.0; $[Ru(III)] = 1.0 \times 10^{-4}$ M).

accounts for the data involves the assumption that there is significant formation of both $[Ru(Me_2Im\text{-}C)^{3+}\cdot NCS^-]$ and $[Ru(Me_2Im\text{-}C)^{3+}\cdot 2NCS^-]$ as labile (outer-sphere) complexes and that there is an activated complex of composition corresponding to each of these:

$$Ru(Me_2Im\text{-}C)^{3+} + NCS^- \overset{K}{\rightleftharpoons} [Ru(Me_2Im\text{-}C)\cdot NCS]^{2+} \xrightarrow{k} Ru(Me_2Im\text{-}C)(NCS)^{2+}$$

$$[Ru(Me_2Im\text{-}C)\cdot NCS]^{2+} + NCS^- \overset{K'}{\rightleftharpoons} [Ru(Me_2Im\text{-}C)\cdot(NCS)_2]^{+} \xrightarrow{k'} Ru(Me_2Im\text{-}C)(NCS)^{2+} + NCS^-$$

The corresponding rate law is

$$\frac{d}{dt}[Ru(Me_2Im\text{-}C)(NCS)^{2+}] = \frac{kK[NCS^-] + k'KK'[NCS^-]^2}{KK'[NCS^-]^2 + K[NCS^-] + 1}[Ru(Me_2Im\text{-}C)^{3+}]$$

where $Ru(Me_2Im\text{-}C)^{3+}$ in the rate law represents the total aquoruthenium(III). The initial slope in a plot of k_{obsd} vs. $[NCS^-]$ is then $kK = 1.9 \times 10^{-1}\ M^{-1}\ s^{-1}$ (with the assumption of a zero intercept), and the intercept of k_{obsd}^{-1} vs. $[NCS^-]$ (Figure 1b) at the high $[NCS^-]$ yields $k' = 1.7 \times 10^{-2}\ s^{-1}$. In principle, it should be possible to treat the data to obtain values of K and K', but their accuracy is not high enough to warrant the more detailed analysis.

Acid Dissociation Constants. When base is added to a solution containing a C-bound complex of Ru(III), the LMCT bands are shifted, and these shifts are reversed by acid. The absorbance changes were used to determine the values of pK_a. When values of $\log[(A - A_H)/(A_{OH} - A)]$ (where A is the observed absorbance, A_H is the limiting value at high acidity, and A_{OH} is the limiting value at low acidity, all taken at a fixed wavelength) are plotted vs. pH, the intercept yields the value of pK_a and the slope is related to the number of protons dissociating (the latter was found to be 1.00 ± 0.05 in all cases we studied). All reactions, except as mentioned below, proved to be reversible, and the spectra showed isosbestic points as pH was changed. The pK_a values thus obtained are listed in Table II. The pK_as of Im, ImH^+, and $(NH_3)_5RuH_2O^{3+}$ are included for comparison. When $Ru(Im\text{-}N)^{3+}$ is deprotonated, the LMCT band shifts to lower energy with enhanced intensity. On the strength of the observation that $Ru(N\text{-}MeIm\text{-}N)^{3+}$ undergoes no analogous color change,[3] the spectral change has been attributed to deprotonation at the pyrrole nitrogen. When $Ru(Im\text{-}C)^{3+}$ is titrated with OH^-, absorption shifts to higher energy and the intensity diminishes; these observations are consistent with deprotonation at coordinated water. The spectral changes for the carbon-bound derivatives $Ru(Im\text{-}C)^{3+}$ and $Ru(Me_2Im\text{-}C)^{3+}$ were fully reversible up to pH ~8.5, but above these values an irreversible decrease in visible absorption occurred concomitant with an increase in the UV. The rate of change in absorption appeared to be first order in $Ru(OH)(Me_2Im\text{-}C)^{2+}$ and increased sharply with pH. The rates as followed at 300 nm and at 550 nm were different, and the spectra of reacting solutions showed isosbestic points only at pH 8.8. The observations indicate a complex reaction sequence or combination of competing reactions, among which reactions 1 and 2, isomerization and disproportionation, are likely possibilities. Reaction 2 is known to occur for certain (π-acid)ruthenium ammines.[18]

Table II. pK_a Values for Ruthenium Imidazole Complexes and Ligands at 25 ± 0.2 °C

	pK_a	main abs band	
		acid	base
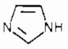	14.2^a		
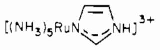	7.06^a		
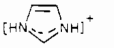	8.9^b ($\mu = 0.10$)	430 (250)	550 (350)
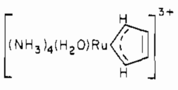	6.9^c ($\mu = 0.10$)	485 (1650)	425 (1750)
$[(NH_3)_5RuH_2O]^{3+}$	4.1^d	...	...
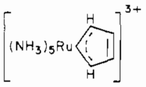	11.0 ($\mu = 3.0$)	483 (900)	589 (1300)

[a] Reference 1. [b] Reference 3, duplicated at $\mu = 0.10$ in this work. [c] $pK_a(Ru(Me_2Im\text{-}C)^{3+}) = pK_a(Ru(Im\text{-}C)^{3+})$ within experimental reproducibility of ±0.1. [d] Reference 15.

$$[(OH)Ru(Me_2Im\text{-}C)]^{2+} \xrightarrow{OH^-} [(OH)Ru(Me_2Im\text{-}N)]^{2+} \quad (1)$$

$$2Ru^{III}(Me_2Im\text{-}C) \xrightarrow{OH^-} Ru^{IV}(Me_2Im\text{-}C) + Ru^{II}(Me_2Im\text{-}C) \quad (2)$$

These complications were circumvented by treating a 3.9×10^{-4} M solution of $Ru(Im\text{-}C)^{3+}$ or $Ru(Me_2Im\text{-}C)^{3+}$ with 3.6 M NH_4^+–NH_3 buffer at pH 8.5. This resulted in a rapid change of the spectrum due to conversion of the aquo to the hydroxo species, followed by a somewhat slower change to a spectrum resembling the parent aquo ion, leading us to formulate the final products as $(NH_3)_5Ru(Im\text{-}C)^{3+}$ or $(NH_3)_5Ru(Me_2Im\text{-}C)^{3+}$. Consistent with these assignments is the replacement of a pK_a near 7 with one now measured as 11.0 and the absence of irreversible changes in the pH 8–10 region. In addition, the band shift on deprotonation is now

---

(18) Rudd, DeF. P.; Taube, H. *Inorg. Chem.* **1971**, *10*, 1543.

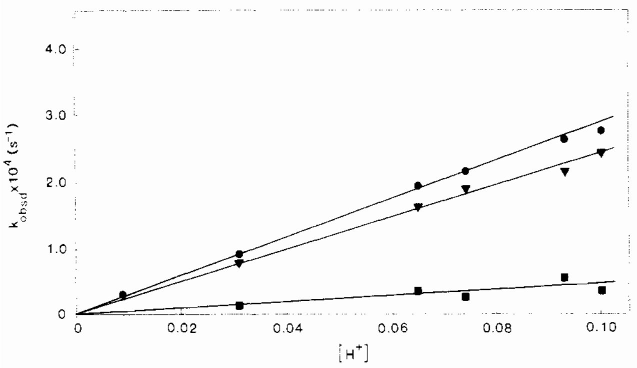

Figure 2. Acid-assisted aquation and isomerization of $(NH_3)_5$Ru-(Hist-*N*)$^{2+}$. The line defined by ● covers the total rate; those defined by ■ and ▼ cover the reactions producing $(NH_3)_5RuH_2O^{2+}$ and Ru(Hist-*C*)$^{2+}$, respectively.

to lower energy and increased intensity, and we attribute the shift to deprotonation at one of the equivalent nitrogens on the carbon-bound imidazolium ligand. At [OH$^-$] = 0.01 M, the carbon-bound pentaammines decompose irreversibly with loss of visible absorption and growth of a strong band at 265 nm, presumably due to the parent ruthenium(II) ion produced by reaction 2. When isn is added to a Ru(Me_2Im-*C*)–NH_3 solution undergoing this change, a band appears in the visible, diagnostic for Ru(Me_2Im-*C*)(isn)$^{2+}$.

None of the ruthenium(II) ions showed significant spectral modification in 0.01 N NaOH, which suggests that their pK_a values are above 12. A similar result was obtained by Sundberg and Gupta[6] for the ions [Ru(Hist-*C*)(CO)]$^{2+}$ and [Ru(Me_2Im-*C*)(CO)]$^{2+}$; their pH titrations revealed no pK_as attributable to imidazole N–H ionization over the pH ranges 3–10.5 and 3–11, respectively.

Ruthenium(II) Species. Acid-Assisted Aquation–Isomerization Reactions. Sundberg et al.[3] found that aquation of Ru(Im-*N*)$^{2+}$ obeys the rate law d[Ru(Im-*N*)$^{2+}$]/d*t* = k[H$^+$][Ru(Im-*N*)$^{2+}$] with $k = 1.18 \times 10^{-2}$ M^{-1} s^{-1} and that at least one competing reaction produced Ru(Im-*C*)$^{2+}$ in 4–12% yield. In a subsequent study[6] [Ru(Hist-*C*)(Cl)]Cl_2 was isolated after solutions of Ru(Hist-*N*)$^{2+}$ were acidified and then oxidized with air. Most (90%) of the total ruthenium was accounted for by [Ru(Hist-*N*)]Cl_3 (40%), [Ru(Hist-*C*)-(Cl)]Cl_2 (50%), and $(NH_3)_5RuCl^{2+}$.[6] These results suggested a rather clean reaction and a competitive edge for isomerization over aquation when histidine is the ligand. We have repeated the kinetic measurements (with some modification) on Ru(Im-*N*)$^{2+}$ and extended them to imidazole derivatives.

Irreversible spectral changes corresponding to loss of Ru-(Hist-*N*)$^{2+}$ (280 nm) and formation of Ru(Hist-*C*)$^{2+}$ (265 nm) are observed when solutions of Ru(Hist-*N*)$^{2+}$ are acidified. An isosbestic point is maintained throughout the course of reaction; at pH 3.15 this occurs at 277 ± 2 nm. The reaction was continuously monitored at 265 nm under pseudo-first-order conditions as a function of acid concentration and found to be first order in Ru(Hist-*N*)$^{2+}$ and H$^+$. The data are summarized in Table III and plotted as k_{obsd} vs. [H$^+$] in Figure 2. The final spectrum was that of Ru(Hist-*C*)$^{2+}$, which on oxidation with ferric ion is converted to Ru(Hist-*C*)$^{3+}$. The total absorbance at 265 nm before oxidation, however, was only 85% of that expected for complete conversion of Ru-(Hist-*N*)$^{2+}$ to Ru(Hist-*C*)$^{2+}$, showing that there is another reaction and that its product absorbs less strongly at 265 nm than does Ru(Hist-*C*)$^{2+}$. For a determination of the products 3.6 μmol of Ru(Hist-*N*)$^{2+}$, 1.20×10^{-3} M in 0.10 N HCl, was allowed to react through 3 half lives and then quenched by air oxidation and eluted from a Sephadex cation-exchange column. A solution of 0.15 N HCl eluted 0.53 μmol of $(NH_3)_5RuCl^{2+}$ (14.7%), which was identified by its absorption at 326 nm (ϵ = 1890). When [HCl] was raised to 0.2 N, 1.6 μmol of Ru(Hist-*C*)$^{2+}$ (44%) was eluted followed by merging bands for Ru(Hist-*N*)$^{3+}$ and a third pink product which forms when C-bound species are oxidized by oxygen (vide infra) but not when ferric ion is used. It should be mentioned that Ru(Hist-*C*)$^{2+}$ in 0.10 N HTFMS aquates only *very* slowly ($k_{obsd} \leq 10^{-7}$ s^{-1}).

Table III. Kinetic Data for Ru(II) at 25.0 ± 0.2 °C and μ = 0.10; [Ru(III)] = (1.0–2.0) × 10^{-4} M

A. Acid-Assisted Aquation and Isomerization

Ru(Im-*N*)$^{2+}$

10^3[H$^+$], M	$10^5 k_{obsd}$,[a] s^{-1}	R_{aq}[b]	$10^5 \times k_{obsd}R_{aq}$, s^{-1}
1.41	3.65	0.96	3.50
9.33	15.7	0.92	14.4
29.0		0.97	
79.4	118	0.97	115
107	160		

Ru(Hist-*N*)$^{2+}$

10^3[H$^+$], M	$10^5 k_{obsd}$, s^{-1}	R_{ism}[b]	$10^5 \times k_{obsd}R_{ism}$, s^{-1}
182 (μ = 0.20)	55.3	0.87	48.1
98.0 (μ = 0.20)	30.8		
9	3.33[d]		
31	9.12	0.87	7.93
65	19.5	0.83	16.2
74	21.7	0.88	19.1
93	26.3	0.80	21.0
100	27.4	0.88	24.1

Ru(Me_2Im-*N*)$^{2+}$

$10^3 \times$ [H$^+$], M	$10^3 k_{obsd}$, s^{-1}	R_{aq}[b]	$10^3 \times k_{obsd}R_{aq}$, s^{-1}
9	2.5 ± 0.8	0.79	2.0
12	29.1 ± 5	0.80	23
40	105 ± 2	0.84	88

Ru(*N*-MeIm-*N*)$^{2+}$

$10^2 \times$ [H$^+$], M	$10^4 \times k_{obsd}$, s^{-1}	$10^2 \times$ [H$^+$], M	$10^4 \times k_{obsd}$, s^{-1}
1.2	1.6	4.0	5.0
2.0	2.6		

B. Formation of Ru(Hist-*N*)$^{2+}$ from $(NH_3)_5RuH_2O^{2+}$ and Hist

$10^2 \times$ [HistH$^+$],[c] M	$10^5 \times k_{obsd}$,[d] s^{-1}	pH	$10^2 \times$ [Hist],[e] M	$10^3 \times k_{obsd}$, s^{-1}	pH
4.3	3.4	3.30	3.97	3.51	7.94
14.4	11.1	3.27	1.89	1.65	7.96

[a] [NCpy + NCpyH$^+$] = 0.10 used as a scavenger, μ = 0.20. [b] R_{aq} and R_{ism} represent the fraction of the product appearing as the aquated and isomerized products, respectively. [c] [Hist$H_2$$^{2+}$] = 0.04[HistH$^+$]. [d] By initial-rate method. [e] [Hist$^-$] = 0.015[Hist].

This work (and the earlier work by Sundberg et al.[3]) suggests that the kinetics can be followed by taking account of processes 3 and 4, the reverse reactions being negligible.

$$\text{Ru(Hist-}N)^{2+} + H^+ \rightarrow \text{Ru(Hist-}C)^{2+} + H^+ \qquad (3)$$

$$\text{Ru(Hist-}N)^{2+} + H^+ \rightarrow RuH_2O^{2+} + \text{HistH}^+ \qquad (4)$$

The specific rate k_{obsd} is given by $(k_3 + k_4)$[H$^+$], where the dissection into k_3 and k_4 will depend on product analysis. The species $(NH_3)_5RuH_2O^{2+}$ and Ru(Hist-*C*)$^{2+}$ both absorb at 265 nm. The assumption that the initial Ru(Hist-*N*)$^{2+}$, Ru(II), results in two products

$$[\mathrm{Ru(II)}] = [\mathrm{Ru(Hist}\text{-}C)^{2+}] + [(\mathrm{NH_3})_5\mathrm{RuH_2O^{2+}}]$$

and the application of the Beer–Lambert relationship to each species in the product solution leads to the equation

$$[\mathrm{Ru(Hist}\text{-}C)^{2+}] = \frac{A - [\mathrm{Ru(II)}]\epsilon_1}{\epsilon_2 - \epsilon_1}$$

A is the observed absorbance and ϵ_1 and ϵ_2 are the extinction coefficients for $(NH_3)_5RuH_2O^{2+}$ and $Ru(Hist\text{-}C)^{2+}$, respectively. The values of the extinction coefficients are listed in Table VI.

$[Ru(Hist\text{-}C)^{2+}]/[Ru(II)]$ is the fraction, R_{ism}, undergoing isomerization and

$$k_3[\mathrm{H^+}] = k_{\mathrm{obsd}}R_{\mathrm{ism}}$$

From the slope of $k_{\mathrm{obsd}}R_{\mathrm{ism}}$ vs. $[H^+]$, plotted as triangles in Figure 2, k_3 was found to be 2.4×10^{-3} M^{-1} s^{-1}. The difference $k_{\mathrm{obsd}} - k_3[H^+]$ yielded the third line in Figure 2, $k_4[H^+]$ vs. $[H^+]$, and from its slope $k_4 = 3.1 \times 10^{-4}$ M^{-1} s^{-1}. It should be noted that the least-squares treatment of the data for the overall reaction leads to an intercept corresponding to a specific rate of 1.1×10^{-5} s^{-1} for an acid-independent path. It is known that isomerization by a path zero order in $[H^+]$ is $<10^{-7}$ s^{-1}. From the equilibrium quotient and the rate of the forward reaction, the specific rate for aquation of the ligand at $[H^+] = 0$ is 2.9×10^{-8} s^{-1}. We conclude therefore that the nonzero intercept reflects a systematic error in the data—perhaps a consequence of slow oxidation—and the lines have been drawn through the origin.

To address the question of whether the isomerization is intra- or intermolecular, we measured the rate of formation of $Ru(Hist\text{-}N)^{2+}$ from $(NH_3)_5RuH_2O^{2+}$ and $HistH^+$. The data are listed in Table III. Needed for their interpretation are the pK_a values for histidine. These are

$$[2+] \xrightarrow{1.9} [1+] \xrightarrow{6.1} [0] \xrightarrow{9.1} [1-]$$

The "extra" final absorption at 265 nm for the experiment with $[HistH^+] = 0.043$ showed that only 7% of $Ru(Hist\text{-}C)^{2+}$ was formed, with the bulk of product absorbing at 280 nm, as appropriate for $Ru(Hist\text{-}N)^{2+}$. The specific rate of product formation was calculated to be 7.64×10^{-4} M^{-1} s^{-1}; 7% of this is 5.4×10^{-5} M^{-1} s^{-1}. Thus, the specific rate of formation of $Ru(Hist\text{-}C)^{2+}$ by the intermolecular path as a primary reaction

$$(\mathrm{NH_3})_5\mathrm{RuH_2O^{2+}} + \mathrm{HistH^+} \rightarrow (\mathrm{NH_3})_5\mathrm{Ru(Hist}\text{-}C)^{2+} + \mathrm{H^+}$$

under the conditions of the isomerization experiments, where $[Hist] \approx 0$ and $[HistH^+] < 10^{-4}$ M, must be less than 10^{-8} s^{-1}, much less than typical values of k_{obsd} under these conditions (10^{-4} s^{-1} and higher).

With use of the equilibrium quotient for protonation of Hist ($\log K_a = 6.1$ at $\mu = 0.15$[1]) in conjunction with the above measured rates of formation and aquation, the equilibrium quotient governing formation of $Ru(Hist\text{-}N)^{2+}$ from Hist and $(NH_3)_5RuH_2O^{2+}$ is calculated as 3.1×10^6 ($\mu = 0.10$).

The air sensitivity and slow rate made the measurement of the rate of loss of histidine by aquation from $Ru(Hist\text{-}C)^{2+}$ impractical. Nevertheless, an upper limit of 10^{-7} s^{-1} could be set at $[H^+] = 0.10$ M from observations after 10 h. Equations 5–8 summarize the known interactions of histidine with the pentaammineruthenium(II) ion, with rate data being given in Chart II. Note that following isomerization, reaction 7, NH_3 is lost from the trans position.

$$(\mathrm{NH_3})_5\mathrm{RuH_2O^{2+}} + \mathrm{Hist} = \mathrm{Ru(Hist}\text{-}N)^{2+} \tag{5}$$

$$(\mathrm{NH_3})_5\mathrm{RuH_2O^{2+}} + \mathrm{HistH^+} = \mathrm{Ru(Hist}\text{-}N)^{2+} + \mathrm{H^+} \tag{6}$$

$$\mathrm{Ru(Hist}\text{-}N)^{2+} + \mathrm{H^+} = \mathrm{Ru(Hist}\text{-}C)^{2+}\ (+\mathrm{NH_4^+}) \tag{7}$$

$$\mathrm{Ru(Hist}\text{-}C)^{2+} + \mathrm{H^+} = (\mathrm{NH_3})_4\mathrm{Ru(H_2O)_2}^{2+} + \mathrm{HistH^+} \tag{8}$$

Chart II. Rate Data for Reactions 5–8

reacn no., n	k_n, M^{-1} s^{-1}	k_{-n}	K_n
5	8.9×10^{-2}	2.9×10^{-8} s^{-1}	3.1×10^{6}
6	7.6×10^{-4}	3.1×10^{-4} M^{-1} s^{-1}	2.4
7	2.4×10^{-3}	$<10^{-6}$ s^{-1}	$>2.4 \times 10^{3}$
8	$\leqslant 10^{-6}$		

The measurement of acid-assisted aquation of $Ru(Im\text{-}N)^{2+}$ was complicated by side reactions in the second half-life, necessitating an analysis of the initial rate data, but a product analysis indicated 95% of the reaction was accounted for by aquation and isomerization.[3] We therefore repeated the measurements using 4-cyanopyridine as a scavenger for both aquated and isomerized products. The rate constants for formation of product in reactions 9 and 10 are $k_9 = 2.6 \times 10^{-1}$ M^{-1} s^{-1} and $k_{10} = 2.4 \times 10^{-1}$ M^{-1} s^{-1}.[19]

$$(\mathrm{NH_3})_5\mathrm{RuH_2O^{2+}} + \mathrm{NCpy} \rightarrow (\mathrm{NH_3})_5\mathrm{RuNCpy^{2+}} \tag{9}$$

$$(\mathrm{NH_3})_5\mathrm{RuH_2O^{2+}} + \mathrm{NCpyH^+} \rightarrow (\mathrm{NH_3})_5\mathrm{RuNCpyH^+} \tag{10}$$

$Ru(Im\text{-}C)^{2+}$ reacts much more rapidly with π acids than does $(NH_3)_5RuH_2O^{2+}$. Under conditions where the acid-mediated aquation and rearrangement of $Ru(Im\text{-}N)^{2+}$ were rate determining, the growth of absorption in the visible region for the products of 9 and 10 led to the determination of pseudo-first-order rate constants from ln $(A - A_\infty)$ vs. time plots (these were linear through at least 3 half-lives). The rate profile as a function of $[H^+]$ is linear with a slope of 1.49×10^{-2} M^{-1} s^{-1} and a near-zero intercept of 1.7×10^{-5} s^{-1}. The difference in the absorbances of $(NH_3)_5RuNCpyH^{3+}$ (532 nm; $\epsilon = 1.26 \times 10^4$) and $Ru(Im\text{-}C)(NCpyH)^{3+}$ (560 nm; $\epsilon = 1.03 \times 10^4$) at 532 nm was used to calculate R_{aq}, the fraction undergoing aquation. Analysis of the kinetic plots by the method used above for the $Ru(Hist\text{-}N)^{2+}$ case yielded the rate constant for acid-assisted aquation (k_{aq}) as 1.43×10^{-2} M^{-1} s^{-1} ($\mu = 0.20$) and for acid-assisted isomerization as 6×10^{-4} M^{-1} s^{-1} ($\mu = 0.20$). The acid-assisted specific rate of aquation has been reported[3] as 1.18×10^{-2} M^{-1} s^{-1} ($\mu = 0.10$). The present results are in accord with the trend to a greater aquation rate at increased ionic strength. For reaction 11 the value of K_{11} was calculated by Sundberg et al.[3] as 2.8×10^6 ($\mu = 0.10$). Using the k_{aq} value from the present work yields $K_{11} = 2.3 \times 10^6$ ($\mu = 0.20$).

$$(\mathrm{NH_3})_5\mathrm{RuH_2O^{2+}} + \mathrm{Im} = (\mathrm{NH_3})_5\mathrm{Ru(Im}\text{-}N)^{2+} \tag{11}$$

The reactions consuming $Ru(Me_2Im\text{-}N)^{2+}$ were much faster than for the other complexes studied and were measured on the stopped-flow instrument. Values of k_{obsd} were determined for 3 half-lives, and plots of k_{obsd} vs. $[H^+]$ and $k_{\mathrm{obsd}}R_{\mathrm{aq}}$ vs. $[H^+]$ were linear with zero intercepts. R_{aq}, the fraction undergoing aquation, was determined spectrophotometrically by the data analysis outlined for the histidine complex. Since the complex $Ru(Me_2Im\text{-}C)^{3+}$ has strong absorption in the visible region, this method (I) could be checked by another analytical method (II). Acid-equilibrated samples were oxidized with ferric ion, and the absorbance was measured at 603 nm, where absorption by $(NH_3)_5Ru(H_2O)^{2+}$ is negligible. Agreement between the two methods was within 4%. For experiments with $[Ru(Me_2Im\text{-}N)^{2+}] = 3.20 \times 10^{-4}$ M, R_{aq} was found by method I to be 0.95, 0.89, 0.81, and 0.78 at [HTFMS] = 0.124, 0.071, 0.014, and 0.001 M, respectively. The linear R_{aq} vs. [HTFMS] relationship was used as a calibration curve to obtain R_{aq} for the kinetic experiments. It is noteworthy that R_{aq} for $Ru(Me_2Im\text{-}N)^{2+}$, which we assume is more accurately determined

---

(19) Allen, R. J.; Ford, P. C. *Inorg. Chem.* **1972**, *11*, 679.

(20) Isied, S. S.; Taube, H. *Inorg. Chem.* **1976**, *15*, 3070.

Table IV. Kinetic Data for Substitution on $Ru(Me_2Im\text{-}C)^{2+}$ [a]

10^2[isn], M	k_{obsd}, s^{-1}	10^4[$Mepyr^+$]	10^3k_{obsd}, s^{-1}
1.05	1.46	3.7	8.5
2.05	2.60	14.6	24.0
5.10	6.80	32.3	49.8
10.3	12.1		
[NCS^-], M	k_{obsd}, s^{-1}	[NCS^-], M	k_{obsd}, s^{-1}
2.31	5.2	16.2	25.5
4.25	7.0	22.6	33.4
6.46	10.6	32.3	43.4
9.69	13.2		

[a] $[Ru(Me_2Im\text{-}C)^{2+}] \leqslant 10[L]$; at 25.0 °C and $\mu = 0.10$, pH 7.0.

than for the much slower reacting analogues, $Ru(Hist\text{-}N)^{2+}$ and $Ru(Im\text{-}N)^{2+}$, is not independent of acid.

The calculated slope of the k_{obsd} vs. $[H^+]$ plot was 2.64 M^{-1} s^{-1}. From it and R_{aq}, k_{aq} and k_{ism} were calculated to be 2.2 and 0.4 M^{-1} s^{-1}, respectively.

In an attempt to synthesize $Ru(N\text{-}MeIm\text{-}C)^{3+}$, a previously unreported derivative, we mixed the ligand (~0.07 M) with $(NH_3)_5RuH_2O^{2+}$ in water. The spectrum after 10 min was that of $Ru(N\text{-}MeIm\text{-}N)^{2+}$ and was stable. When the solution was diluted with deoxygenated acid, the ion aquated to $(NH_3)_5RuH_2O^{2+}$ and, presumably, free $N\text{-}MeImH^+$. The rate data, though approximate, are included in Table III. The calculated specific rate is $k_{obsd}/[H^+] = 1.2 \times 10^{-2}$ M^{-1} s^{-1}. The final absorbance at 262 nm was within 2% of that expected for $(NH_3)_5RuH_2O^{2+}$. Either no carbon-bound isomer had formed or it had aquated rapidly.

Substitution on $Ru(Me_2Im\text{-}C)^{2+}$. The trans-aquo position of $Ru(Me_2Im\text{-}C)^{2+}$ is substituted rapidly by L = NCS^-, isn, Im, and $Mepy^+$. Spectra of the products are summarized in Table VI.

Experiments with isn as entering ligand were conducted in isn solutions titrated to pH 7.0, where the ruthenium(II) complex is in the aquo form and isn is in the unprotonated form ($pK_a = 3.85$). Contributions from subsidiary paths involving protonated ligand are thus avoided.

The specific rate governing the approach to equilibrium in the reaction

$$Ru(Me_2Im\text{-}C)^{2+} + isn \rightarrow Ru(Me_2Im\text{-}C)(isn)^{2+} \quad (12)$$

takes the form

$$k_{obsd} = k_{12}[isn] + k_{-12}$$

The rate was measured at 470 nm under pseudo-first-order conditions, isn in excess, the data being summarized in Table IV. The values reported are the average of replicate determinations made on the stopped-flow apparatus. A plot of k_{obsd} vs. [isn] shows a clean first-order dependence on [isn], the slope yielding $k_{12} = 1.13 \times 10^2$ M^{-1} s^{-1}. A small intercept can be ascribed to incomplete reaction, but its value is not accurately determined by these data. However, the equilibrium quotient regulating complexation was small enough to be determined by spectrophotometric titration. The value thus obtained is $K_{12} = (7.2 \pm 0.2) \times 10^2$, and the reverse rate k_{-12} then is fixed at 0.16 s^{-1}.

The method adopted for NCS^- as ligand followed that described above for the isn reaction, and the observations are summarized in Table IV. The forward and reverse specific rates are 1.33×10^4 M^{-1} s^{-1} and 1.95 s^{-1}, respectively. The corresponding equilibrium quotient is then calculated to be 6.8×10^3.

Substitution rates for $Mepyr^+$ as ligand were slow enough to measure on the spectrophotometer. The forward and reverse rates as obtained from a plot of the data in Table IV are 1.45×10 M^{-1} s^{-1} and 3.1×10^{-3} s^{-1}, respectively.

Im as entering ligand failed to compete measurably with isn under the conditions $[isn] = [Im] = [ImH^+] = 0.01$ M. If it is assumed that the failure to react is not a matter of affinity, the specific rate of the substitution by Im is at most 0.1 times that by isn, or <11 M^{-1} s^{-1}.

A single experiment was done with isn as entering ligand but with $Ru(Im\text{-}C)^{2+}$. The specific rate measured with [isn] = 0.10 M is 7.5 s^{-1}. A previous investigation[20] led to $k_f = (7.4 \pm 2.1) \times 10$ M^{-1} s^{-1}, $k_r = 1.2 \times 10^{-1}$ s^{-1}, and $K_{eq} = 6 \times 10^2$ for this reaction.

Oxidation–Reduction Potentials. Cyclic voltammetry measurements for a series of the N-bound pentaammine and C-bound tetraammine ions yielded the Ru(III)/Ru(II) formal reduction potentials recorded in Table V. Interpretation of the results is for the most part straightforward. An exception, the $Ru(Me_2Im\text{-}C)(isn)$ ion, is discussed below.

The trend as the ligand is derivatized, to more oxidizing potentials in the order E_f for $(-CH_3)_2 < (-H)_2 <$ phenyl is expected; as the ligand becomes increasingly electrophilic, Ru(II) is stabilized relative to Ru(III). A more striking effect emerges when N-bound vs. C-bound complexes are compared. Replacing two methyl substituents by an aromatic in the ligand stabilizes Ru(II) over Ru(III) by 0.07 V when the ligand is N-bound and 0.225 V when it is C-bound. It should be mentioned that a correlation between $E_f((NH_3)_5RuL^{3+/2+})$ and $E_f(trans\text{-}(NH_3)_4Ru(H_2O)L^{3+/2+})$ is linear[21] and that E_f for the aquotetraammine[2] of $Ru(Im\text{-}N)^{3+/2+}$ is found to be the same as for $Ru(Im\text{-}N)^{3+/2+}$.

In the measurement of the formal potential for $Ru(Me_2Im\text{-}C)(isn)^{3+/2+}$, the complex was generated in situ by adding $Ru(Me_2Im\text{-}C)^{2+}$ to a 0.20 M isn–$isnH^+$ buffer made with HTFMS at pH 3.90, so that $[Ru(Me_2Im\text{-}C)(isn)^{2+}] = 1 \times 10^{-3}$ M. The cyclic voltammogram for this solution showed one oxidation wave with the current maximum at 0.328 V and two reduction waves, at 0.255 and 0.164 V. The reduction waves were of equal amplitude at a scan rate of 0.05 V s^{-1}, but as the scan rate was increased, the more reducing wave diminished, until, at 1.0 V s^{-1}, it was only a small inflection to the reducing side of what appeared to be a reversible couple, $E_f = 0.295$ V, with an anodic–cathodic peak potential difference of 0.060 V. We take 0.295 V to be the formal potential of $Ru(Me_2Im\text{-}C)(isn)^{2+/3+}$. The extra reduction wave falls at a position corresponding to the process

$$Ru(Me_2Im\text{-}C)^{3+} + e^- \rightarrow Ru(Me_2Im\text{-}C)^{2+}$$

The lack of a feature resulting from the reverse of the above is consistent with the rapid substitution by isn of H_2O, which, at [isn] = 0.10 M, is governed by a rate constant of 11 s^{-1}. Roughly 25% of the $Ru(Me_2Im\text{-}C)(isn)^{3+}$ formed by the oxidation scan was lost during 20 s of scanning. Thus k_{obsd} for the approach of $Ru(Me_2Im\text{-}C)(isn)^{3+}$ to aquation equilibrium is approximately 1.7×10^{-2} s^{-1}. The equilibrium quotient governing the ligation of $Ru(Me_2Im\text{-}C)^{3+}$ by isn was calculated above (see Ruthenium(III) Complexes) to be 1.2. With the relation

$$k_r = \frac{k_{obsd}}{K_{eq}[isn] + 1}$$

k_r and k_f can be calculated, given the value of k_{obsd} at known [isn]. The value of $k_{obsd} = 1.7 \times 10^{-2}$ when [isn] = 0.10 M leads to $k_r = 1.5 \times 10^{-2}$ s^{-1} and $k_f = 1.8 \times 10^{-2}$ M^{-1} s^{-1}.

Electronic Spectra of *trans*-$L(NH_3)_4RuL'$ Species. In the foregoing, the observations that have led to our conclusion about the state of the ru(II) and Ru(III) species in different environments were described. In Table VI are summarized

---

[21] Tweedle, M. F., unpublished results.

Table V. Reduction Potentials[a] vs. NHE for Imidazoliumruthenium(II, III) Ammine Complexes

	E_f (pp),[b] V		E_f (pp),[b] V
Ru(Me$_2$Im-*N*)	0.090 (0.100)[c]	Ru(Me$_2$Im-*C*)	0.130 (0.075)
Ru(Im-*N*)	0.115 (0.070)	Ru(Im-*C*)	0.210 (0.080)
Ru(BzIm-*N*)	0.155 (0.065)	Ru(BzIm-*C*)	0.365 (0.065)
Ru(Me$_2$Im-*C*)(isn)	0.295 (0.060)[d]	Ru(Im-*C*)(NCS)	0.130 (0.060)[e]
Ru(Me$_2$Im-*C*)(NCS)	0.090 (0.088)[e]	*trans*-(H$_2$O)(NH$_3$)$_4$Ru(Im-*N*)	0.120 (0.075)

[a] ±0.005 V; measured at a Pt-button electrode at 22 °C in 0.10 N HTMS for C-bound complexes and 0.10 N NaTFMS for N-bound complexes. Details are in the Experimental Section. [b] Peak to peak separations (pp) are shown in parentheses. For Ru(NH$_3$)$_6$Cl$_3$ in 0.10 N HTFMS pp = 0.68 V. [c] At a carbon-paste electrode. [d] See text. [e] 0.10 N NaNCS, pH 5.

Table VI. Spectra of *trans*-[L(NH$_3$)$_4$RuL′] Complexes

		λ_{max}, nm (ϵ, M^{-1} cm^{-1})		
L	L′	Ru(II)	Ru(III)	medium[a]
Me$_2$Im-*C*	H$_2$O	265 (9800)	230 (5250), 603 (5100)[b]	0.10 N HTFMS[3]
	OH$^-$		230 (5300), 305 (2400), 513 (2500)	0.10 M Na$_2$CO$_3$-NaHCO$_3$, pH 8.5
	Cl$^-$		322 (1500), 600 (3960)	1.0 M LiCl
	Br$^-$		400 (690), 600 (3800)	1.0 M LiBr
	NCS$^-$	287 (15 500)	440 sh (1600), 606 (5100)	0.10 M NaNCS
	isn	471 (9600)		0.10 M isn, $\mu = 0.10$
	Im-*N*	286 (~3000)		0.10 M Im
	Mepyr$^+$	620 (10 000)		0.10 M MepyrI
Im-*C*	H$_2$O	262 (8350)	224 (5700), 485 (1650)[b]	0.10 N HTFMS[3]
	OH$^-$		425 (1750)	0.10 M Na$_2$CO$_3$-NaHCO$_3$, pH 8.8
	NH$_3$		483 (890)	NH$_3$-NH$_4^+$ (TFMS$^-$), $\mu = 3.5$–4.0
	NCS$^-$		505 (1850)	0.10 M NaNCS
	NCpyH$^+$	560 (10 300)		0.10 M CNpy–CNpyH$^+$ (TFMS$^-$) pH 1.0, $\mu = 0.20$
	isn	462 (8000)		0.10 M isn, $\mu = 0.10$[20]
	CO	220 (15 600)		CO-bubbled aq soln[3]
Im-*C*$^-$	NH$_3$		589 (1300)	NH$_3$-NH$_4^+$ (TFMS$^-$), $\mu = 3.5$–4.0
Hist-*C*	H$_2$O	265 (7200)	229 (6550), 515 (1450)[b]	0.10 N HTFMS[6]
BzIm-*C*	H$_2$O	325, 275, 270, 253, 223	222 (9900), 275 (6800), 485 (660)[b]	0.10 N HTFMS
Im-*N*	NH$_3$	255 (2800), 280 sh (2700)	299 (1880), 430 (250)	0.10 N NaTFMS[3]
Me$_2$Im-*N*	NH$_3$	280 (2820)	312 (2150), 535 (175)	0.10 N NaTFMS[3]
Hist-*N*	NH$_3$	260 (3250), 280 (3150)	301 (2100), 446 (300)	0.10 N NaTFMS[6]
N-MeIm-*N*	NH$_3$	258 (2850), 288 (2650)	312 (2310), 425 (186)	0.10 N NaTFMS[3]
BzIm-*N*	NH$_3$		255 (5900), 262 (5950), 269 (7000), 275 (6300), 443 (1370)	0.10 M NaTFMS[3]
NH$_3$	H$_2$O	262 (540)		0.10 N HTFMS[22]
NH$_3$	NCpyH$^+$	532 (12 560)		0.10 M CNpy–CNpyH$^+$ (TFMS$^-$), pH 1.0, $\mu = 0.20$[19]

[a] Reference number indicates a previous measurement in a different medium. [b] Visible λ_{max} values for tetraammineaquo(2-imidazolium)ruthenium(III) ions are medium sensitive.

the major characteristics of the absorption spectra of the various complexes we have dealt with.

Oxidation of Ru(Me$_2$Im-*C*)$^{2+}$ by Hydrogen Peroxide. Stoichiometry. Exposure of solutions of Ru(Me$_2$Im-*C*)$^{2+}$, 4.4 × 10^{-5} and 1.04 × 10^{-4} M, to 100-fold excess hydrogen peroxide at pH ≤4 produced Ru(Me$_2$Im-*C*)$^{3+}$, quantitatively. The absorbance of Ru(Me$_2$Im-*C*)$^{3+}$ at 600 nm subsequently decayed by a much slower reaction zero order in ruthenium. At lower H$_2$O$_2$:Ru ratios, the yield of Ru(Me$_2$Im-*C*)$^{3+}$ dropped. In Figure 3 are mapped the results of an experiment applying the method of continuous variation[33] to the reaction. Though the end point is close to that expected for a 2:1 Ru:H$_2$O$_2$ stoichiometry, the apparent yields of Ru(Me$_2$Im-*C*)$^{3+}$ were only 75% of theoretical and rereduction restored Ru(Me$_2$Im-*C*)$^{2+}$ (262 nm) in 80% of theoretical yield based upon initial Ru. The Ru(Me$_2$Im-*C*)$^{3+}$–H$_2$O$_2$ solutions before rereduction exuded an odor like that of biacetyl, and when a solution 10^{-3} M in both Ru(II) and H$_2$O$_2$ was eluted on a cation-exchange column (Bio-Rad), the neutral fraction, after concentration on a rotary evaporator, showed a single NMR peak at δ 3.3. This solution was concentrated on a rotary evaporator, yielding an oily solid. Chloroform-*d* dissolved the oil and dissipated most of the odor. D$_2$O dissolved the remaining white solid. The D$_2$O solution showed δ 1.9 (singlet). The NMR of the CDCl$_3$ solution showed a clean singlet at δ 2.3 and a broad multiplet at δ 1.4–0.8. The feature at δ 2.3 is that expected for biacetyl, δ 2.3; reagent biacetyl (Aldrich) shows peaks in the region δ 1.4–0.8, and these are ascribable to impurities.

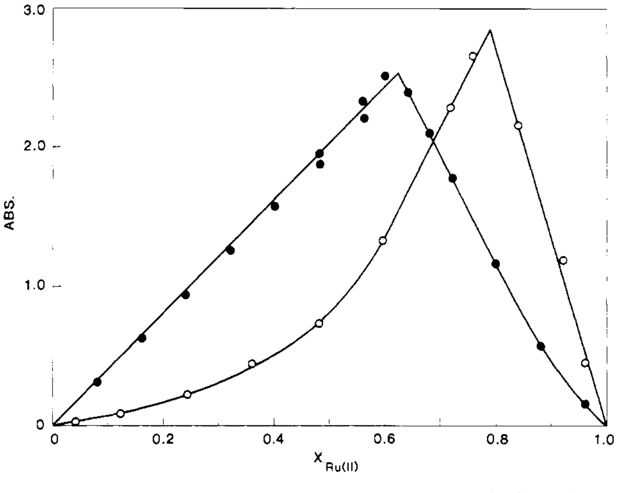

Figure 3. Results of experiments using the method of continuous variations to establish the stoichiometries of the reactions of H$_2$O$_2$ with Ru(Me$_2$Im-*C*)$^{2+}$ (●) and of O$_2$ with Ru(Me$_2$Im-*C*)$^{2+}$ (○) (concentration level 1.0 × 10^{-3} M; 0.10 M HBF$_4$; 25 °C). Absorbance, *A*, was measured at 600 nm. $X_{Ru(II)}$ ≡ mole fraction of Ru(II).

---

(22) Armor, J. N. Ph.D. Thesis, Stanford University, 1970.

Table VII. Observed Rates of Oxidation of $Ru(Me_2Im\text{-}C)^{2+}$ by Hydrogen Peroxide at 25.0 ± 0.2 °C, $\mu = 0.10$ M $HBF_4\cdot$, and $[Ru^{II}(Me_2Im\text{-}C)] = (0.9\text{–}1.1) \times 10^{-4}$ M

$10^3 \times [H_2O_2]$, M	k_{obsd}, s^{-1} [a]	$10^3 \times [H_2O_2]$, M	k_{obsd}, s^{-1} [a]
1.32	3.0[b]	20.0	37 (2.0)
2.11	5.6 (0.2)	25.0	53.5 (0.9)
3.29	7.0[b]	30.0	63 (1.4)
4.22	10.0 (0.3)	35.0	69 (1.5)
6.58	13.9[b]	39.9	83 (2.5)
32.9	70[b]	44.9	88 (2.5)
3.49	8.8 (0.17)	49.9	94[b]
4.99	12.4 (0.4)	2.11	5.9[b] (pH 4.02)
10.0	21.3 (0.5)	5.25	14.2 (0.4) ($[Fe^{2+}] = 5 \times 10^{-5}$ M)
15.0	30 (1.7)	26.3	72 (2.0) ($[Fe^{2+}] = 5 \times 10^{-4}$ M)

[a] From range of k_{obsd} values where multiple determinations were made. [b] Single determination.

Biacetyl ($CH_3COCOCH_3$) is a two-electron oxidized product of acetoin ($CH_3CH(OH)COCH_3$), a starting material in the synthesis of the free ligand, and it is undoubtedly produced by decomposition of the coordinated dimethylimidazolium ligand. Hydrogen peroxide does not perceptibly attack the free ligand under any experimental conditions used in this study, nor does it react with the ruthenium(III) product rapidly enough to significantly affect the yields. The deficiency in $Ru(Me_2Im\text{-}C)^{3+}$ produced is, therefore, best attributed to the action of a reactive intermediate. Likely candidates are OH· and Ru(IV). In attempts to scavenge the intermediate with free ligand (>2 M), I^- (0.1 M), Br^- (0.1 M), and *tert*-butyl alcohol (>3 M), the yield of $Ru(Me_2Im\text{-}C)^{3+}$ was not improved.

Attempts to measure hydrogen peroxide consumed under the concentration conditions needed to conserve the complex failed because of the inherent inaccuracy in such determination at very high ratios of $[H_2O_2]$:[Ru(II)]. Irreproducibility is also ascribable to catalytic decomposition of H_2O_2.[23,24]

Kinetics of the $Ru(Me_2Im\text{-}C)^{2+}$–H_2O_2 Reactions. Concentrations were those appropriate to stopped-flow measurements under pseudo-first-order conditions with hydrogen peroxide in excess. Acidity and ionic strength were controlled with 0.10 M HBF_4 and 0.10 M $NaBF_4$.

Table VII summarizes the observed rates of formation of $Ru(Me_2Im\text{-}C)^{3+}$ measured at 600 nm. The rates were not significantly enhanced by added Fe^{2+} at low concentration or Cl^- and were proton independent in the range pH 1–4. A plot of the data in Table VII shows that k_{obsd} varies directly with $[H_2O_2]$ and yields a slope of $(1.92 \pm 0.05) \times 10^3$ M^{-1} s^{-1} with zero intercept. The specific rate of the rate-determining step

$$Ru(Me_2Im\text{-}C)^{2+} + H_2O_2 \rightarrow$$

is therefore 9.6×10^2 M^{-1} s^{-1} (it is assumed that each act of the rate-determining step accounts for two molecules of Ru(III) being formed). Shigehara and Anson,[27] using $Ru(Hist\text{-}C)^{3+/2+}$ immobilized on an electrode to catalyze the electrolytic reduction of H_2O_2, have observed a rate of 8.6×10^3 M^{-1} s^{-1} for the reduced form of their complex.

Oxidation of $Ru(Me_2Im\text{-}C)^{2+}$ and $RuImC^{2+}$ with Oxygen. The results of a continuous-variation experiment for oxidation of $Ru(Me_2Im\text{-}C)^{2+}$ by molecular oxygen are plotted in Figure 3. In this experiment $[Ru^{2+}] + [O_2] = 1.2 \times 10^{-3}$ M and $[H^+] = 0.10$ M. The yields of $Ru(Me_2Im\text{-}C)^{3+}$ are again low, in this case by ~25%. The maximum in [Ru(III)] is observed at $X_{Ru(II)}$ = mole fraction of Ru(II) = 0.79, close to the theoretical [Ru(II)]:$[O_2]$ ratio of 0.80 for a 4:1 stoichiometry. The plot, however, is distorted by curvature at low $X_{Ru(II)}$, and in addition, an unexpected absorbance appeared at 310 nm that maximized at $X_{Ru(II)} = 0.32\text{–}0.47$. For $Ru(Im\text{-}C)^{2+}$ as reactant, the deficiency in final absorbance was 50% at $X_{Ru(II)} = 0.8$, the new absorbance band had moved to 275 nm, and when the ratio $[O_2]$:$[Ru(Im\text{-}C)^{2+}]$ was larger than 10, less than 0.4% of the reaction proceeded to the $Ru(Im\text{-}C)^{3+}$ product.

In each of a series of attempts to identify the product absorbing at 275 nm (this will hereinafter be referred to as RuP 275), when oxygen in excess acts on $Ru(Im\text{-}C)^{2+}$, a solution of $Ru(Im\text{-}C)^{2+}$ was syringed into a solution through which oxygen was vigorously bubbling. For these experiments $[O_2] = 1.2 \times 10^{-3}$ M, $[Ru]_{final} = (2\text{–}9) \times 10^{-5}$ M, and the pH covered a wide range. The product absorbance showed peaks at 275 (ϵ = 3600) and 510 nm (ϵ = 100) compared to 234 (ϵ = 5700) and 485 nm (ϵ = 1650) for $Ru(Im\text{-}C)^{3+}$ (the values of ϵ are calculated for total Ru). When the final $[Ru(Im\text{-}C)^{2+}]$ is greater than 1×10^{-4} M, the visible absorption of the product solution increases (485 nm for $Ru(Im\text{-}C)^{3+}$) and the 275-nm absorption decreases. The final absorbance at 275 nm is unaffected by pH in the range 1–8 when $[Ru(Im\text{-}C)^{2+}] < 10^{-4}$ M. Bubbling argon through the product solution does not reverse the reactions. Solutions of RuP-275 are fairly stable. Whether the solution is kept under argon or air, the absorbance decreases by only 2–3% in 0.10 M NaTFMS or 0.10 M HTFMS. Attempts to characterize the species using chromatography (Bio-Rad or Sephadex resins) failed because of decomposition. The eluate using 0.3 M HCl shows absorption at 480 and 225 nm, as does $Ru(Im\text{-}C)^{3+}$, but with $\epsilon_{225}/\epsilon_{480}$ twice that of pure $Ru(Im\text{-}C)^{3+}$. Absorption by C-bound imidazole in Ru(III) at 480 nm decreases as NH_3 is replaced by H_2O or by Cl^-. The decrease in the ratio $\epsilon_{225}/\epsilon_{480}$ referred to in the experiments to be described that are devoted to reducing RuP-275 is also attributed to replacement of NH_3 by H_2O. It should be noted that Sundberg et al.[3] reported "extensive deamination" of a small portion of the Ru(II) in solutions containing $Ru(Im\text{-}C)^{2+}$ when air was used as oxidant.

To determine whether RuP-275 has a dissociable proton in an accessible range, we measured the absorption at 275 nm as a function of pH, beginning at 2. A value of $pK_a = 10.2$ was thus determined, rather close to that of $(NH_3)_5Ru(Im\text{-}C)^{3+}$ ($pK_a = 11.0$). The value is too high to be attributed to H_2O associated with Ru(III) or Ru(IV).

The ligand remains attached as, or readily convertible to, the imidazolium form. Deoxygenated solutions of RuP-275 are reduced by excess Eu^{2+} to produce the $H_2ORu(Im\text{-}C)^{2+}$ chromophore, absorbing at 262 nm. Its measured extinction coefficient was 8100 M^{-1} cm^{-1}, 97% of the theoretical 8350 M^{-1} cm^{-1} for $Ru(Im\text{-}C)^{23}$. The solution thus produced was injected under the surface of an oxygen-saturated solution of 0.10 M NaTFMS to reproduce RuP-275 with a yield of 100 ± 10%.

A titration of RuP-275 was performed with europous ion as reducing agent:

$$Eu^{3+}(aq) + e^- = Eu^{2+}(aq) \qquad E^\circ = -0.43 \text{ V (vs. NHE)}^{25}$$

Stock solutions of $[Eu^{3+}] = 1.39 \times 10^{-3}$ M in 0.10 N HTFMS and $[RuP\text{-}275] = 9.0 \times 10^{-5}$ M were prepared on the basis of the weight of Eu_2O_3 (Research Chemicals, 99.99%) and the extinction coefficient of $Ru(Im\text{-}C)^{2+}$. Argon was bubbled continuously through both solutions and Eu^{3+} reduced to Eu^{2+} with zinc amalgam. By experimentation with europous titration of $Ru(Im\text{-}C)^{3+}$ it was found that errors could be kept

---

(23) Bennett, L. E. *Prog. Inorg. Chem.* **1973**, *18*, 1. Walling, C.; Partch, R. E.; Weil, T. *Proc. Natl. Acad. Sci. U.S.A.* **1975**, *72*, 140.

(24) The evolution of gas, presumably O_2, was observed in solutions of $Ru(Me_2Im\text{-}C)^{3+}$ (1.0×10^{-4} M) in the presence of H_2O_2 (3.8×10^{-3} M) on standing.

(25) "Handbook of Chemistry and Physics", 57th ed.; Chemical Rubber Publishing Co.: Cleveland, Ohio, 1976; p D-141.

(26) Bailey, R.; Boltz, D. F. *Anal. Chem.* **1959**, *31*, 117.

(27) Shigehara, K.; Anson, F. C., report in preparation.

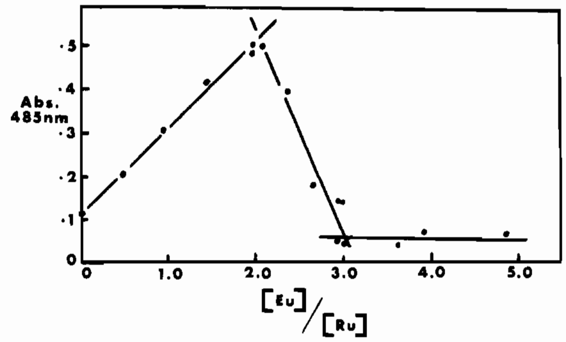

Figure 4. Spectrophotometric titration with Eu^{2+} of a solution of RuP-275. [Ru] = 8.9×10^{-5} M in 0.1 M HTFMS.

Table VIII. Observed Rates of Reaction of Oxygen with $Ru(Im\text{-}C)^{2+}$ at 23.5 °C

$10^4[O_2]$, M	10^2k_{obsd}, s^{-1}	medium[a]
11.0	15.0	0.106 N HTFMS
5.7	7.2	0.106 N HTFMS
2.4	3.0	0.106 N HTFMS
1.2	1.8	0.106 N HTFMS
2.4	2.8	0.10 M NaTFMS, pH 4.53
2.4	4.7	0.100 N HCl
2.4	3.1	0.10 M NaCl, pH 4.25
2.3	0.64[b]	0.10 M NaNCS, pH 1.17 (HTFMS)
11.2	1.8[b]	0.10 M NaNCS, pH 1.20 (HTFMS)

[a] $[Ru(Im\text{-}C)^{2+}] = (0.8\text{–}1.0) \times 10^{-5}$ M. [b] Single determination.

below about 5% for each quantitative transfer of air-sensitive material; a fresh aliquot of RuP-275 was used for each datum, and thus the errors did not accumulate. In Figure 4 is illustrated a spectrophotometrically monitored titration followed at 485 nm. The end points at 2.0 and 3.0 mol of Eu^{2+}/mol of Ru are precise. The spectrum of the product at the first end point showed bands at 485 ($\epsilon = 706$) and 224 nm ($\epsilon = 6000$), compared to 485 ($\epsilon = 1650$) and 224 nm ($\epsilon = 5700$) for $Ru(Im\text{-}C)^{3+}$. After the second end point, the spectrum was that of $Ru(Im\text{-}C)^{2+}$, quantitative within experimental error. The first end point when measured at 275 or 262 nm agreed with that using $\lambda = 485$ nm, but on further addition of Eu^{2+} the data scattered somewhat, giving a second end point at 3.3 ± 0.2 mol of Eu^{2+}/mol of Ru.

Ferrous ion was also used as a reducing agent, excess ferrous ion being added, and the excess then determined[2] as $Fe(phen)_3^{2+}$. The results averaged from three experiments were 0.92 ± 0.03 Fe^{2+} per initial Ru^{2+}.

Kinetics of the $Ru(Im\text{-}C)^{2+}$–O_2 Reaction. The reaction of $Ru(Im\text{-}C)^{2+} + O_2 \rightarrow$ RuP-275 was followed by observing absorbance loss at 262 nm in excess oxygen. The observed pseudo-first-order rate constants are listed in Table VIII. A linear rate profile, k_{obsd} vs. $[O_2]$, demonstrated a clean first-order dependence on $[O_2]$ with a zero intercept and a slope of 1.36×10^2 M^{-1} s^{-1}. (For the reaction of O_2 with $Ru(Hist\text{-}C)^{2+}$, a specific rate of 92 M^{-1} s^{-1} has been obtained.[27]) In view of the results obtained with H_2O_2 as oxidant, we will assume that 4 mol of Ru(II) are consumed for each mole of O_2, so that the specific rate for the determining step is 34 M^{-1} s^{-1}. Within the error limits, ±6%, the reaction is independent of $[H^+]$ over the range $10^{-4} > [H^+] > 10^{-1}$.

Of crucial importance to the mechanism is the reduction in rate by a factor of at least 5 when the medium is 0.10 M in NaNCS so that both oxidation states are complexed. (For these experiments the formation of $Ru(Im\text{-}C)(NCS)^{2+}$ was monitored at 505 nm.) The rate decrease occurs in spite of a driving force larger by 0.08 V, as shown by the formal potentials in Table V. The product is the expected ruthenium(III) NCS^- complex in quantitative yield. By analogy with other "nonlabile" ruthenium(II) ammines, we take the specific rate for the rate-determining step in the oxidation of $Ru(Im\text{-}C)(NCS)^+$ by oxygen to be $k_{obsd}/2[O_2]$. With use of the more accurate air-saturation data, the specific rate is calculated as 13.7 M^{-1} s^{-1}. This rate constant fits on the LFER developed by Stanbury, Haas, and Taube[28] for one-electron outer-sphere oxidations of ruthenium(II) ammines by oxygen. For the $Ru(Im\text{-}C)^{2+}$–O_2 reaction, $k_{obsd}/4$ falls more than 1 order of magnitude to the fast side of the LFER.

Discussion

Where comparisons are possible, it is found that the affinity of a ligand for Ru(III) or Ru(II) is decreased when NH_3 trans to H_2O in the pentaammine complex is replaced by a carbon-bound imidazole. This alone says nothing about whether the bond in the trans position is weakened and only shows that the affinity of the metal for the ligand is reduced relative to that for H_2O. However, in view of the fact that the trans positions are strongly labilized, it is likely that the bond to all trans ligands is weakened when NH_3 is replaced by the imidazolium moiety.

Since back-bonding is not considered to be very important for the Ru(III) state, it might be expected that the affinities for $Ru(Im\text{-}C)^{3+}$ (most of the data were actually obtained for $Ru(Me_2Im\text{-}C)^{3+}$) will closely parallel those for $(NH_3)_5RuH_2O^{3+}$, but with the affinity being lower. In fact, idiosyncrasies appear even among the few data that are available for comparison. Substituting a trans NH_3 in $(NH_3)_5RuH_2O^{3+}$ by $Me_2Im\text{-}C$ lowers the affinity for Cl^- by a factor of 20–100 and for OH^- by a factor of 10^3. In qualitative terms, this difference is reasonable enough because the association quotient for Cl^- with $(NH_3)_5RuH_2O^{3+}$ is $\sim 10^2$ while that for OH^- is 10^{10}.[15] What is surprising is that the affinities for isn[17] and imidazole[3] are brought down from $\sim 1 \times 10^4$ and 3×10^4, respectively, in the case of $(NH_3)_5RuH_2O^{3+}$ to very low values (K_{assoc} for isn is calculated as 1.2 from the redox potential and K_{assoc} for Im appears to be no greater than for the halide ions). Furthermore, in view of the data just cited, the affinity quotient of $Ru(Me_2Im\text{-}C)^{3+}$ for NCS^-, calculated as 3.3×10^4 from the value for the Ru(II) form and the relevant values of E_f, seems remarkably high.

Unfortunately, not many data pertaining to the same nucleophiles are available for other trans-labilizing groups. The single comparison that is possible does little to clarify matters. When SO_3^{2-} replaces a trans NH_3 from $(NH_3)_5RuH_2O^{3+}$, the affinity of Ru(III) for imidazole is reduced by a factor of about 10 but that of isn by a factor of 10^3, the resulting equilibrium quotients being 4.3×10^3 and 8.6, respectively.[29] As noted above, such a strong discrimination in favor of Im-*N* is not shown by $Ru(Me_2Im\text{-}C)^{3+}$.

When the data for carbon-bound imidazole on Ru(II) are considered, the dominant effect, as observed also for SO_3^{2-} and $(RO)_3P$ in the trans position, is that the affinity for a π acid such as isn is drastically reduced as compared to that for the pentaammine case. The association quotient for isn reacting with the latter is 2×10^9;[30] when $Me_2Im\text{-}C$, SO_3^{2-}, and $P(OR)_3$ are in the trans positions, the values of the association quotients are 7.2×10^2, 9,[20] and 36,[31] respectively. The association quotient for $Mepz^+$ reacting with $(NH_3)_5RuH_2O^{2+}$ is likely even greater than for isn. Placing $Me_2Im\text{-}C$ trans to the water reduces the quotient to 4.7×10^3, while $P(OR)_3$ in the same position reduces it to 9.[31] In the two cases in which there are data on which to base comparisons, $P(OR)_3$ is seen to exert a more powerful effect than does $Me_2Im\text{-}C$ in lowering the

---

(28) Stanbury, D. M.; Haas, O.; Taube, H. *Inorg. Chem.* **1980**, *19*, 518.

(29) Brown, G. M.; Sutton, J. E.; Taube, H. *J. Am. Chem. Soc.* **1978**, *100*, 2767.

(30) Taube, H. *Comments Inorg. Chem.* **1981**, *1*, 17.

(31) Franco, D. W.; Taube, H. *Inorg. Chem.* **1978**, *17*, 571.

affinity for a π acid, and in the case of isn vs. $Mepz^+$, it actually reverses the order as compared to substitution in $(NH_3)_5RuH_2O^{2+}$.

The values of pK_a for the Ru(III) complexes merit some comment. In the comparison of ImH^+ ($pK_a = 7.06$) and $(NH_3)_5Ru(Im\text{-}C)^{3+}$ ($pK_a = 11.0$) it should be borne in mind that the species differ only in that in one case a proton and the other $(NH_3)_5Ru^{3+}$ occupies position 2. Because the metal carries a much higher positive charge than the proton, at first sight the result that ImH^+ is the stronger acid appears anomalous. However, the inductive effect of a proton is much greater than that of $(NH_3)_5Ru^{3+}$—note that H_3O^+ is more acidic than $(NH_3)_5RuH_2O^{3+}$ by a factor of $\sim 5 \times 10^5$—and while the inductive effect is attenuated as more atoms intervene between the site of deprotonation and the activating group, it is not surprising that in the present instance the effect of the proton in promoting acidity is greater than that of $(NH_3)_5Ru^{3+}$. The lower value of pK_a for $(NH_3)_5Ru(Im\text{-}N)^{3+}$ (8.9) compared to that for $(NH_3)_5Ru(Im\text{-}C)^{3+}$ (11.0) also is in harmony with arguments based on inductive effect. The arrangement of Ru(III) and H(I) in which H(I) is closer to the site of deprotonation is expected to enhance the acidity more.

The values of E_f show that C-bound imidazole stabilizes Ru(II) compared to Ru(III) somewhat more than the N-bound form does. This difference does not follow readily from first principles, but it does relate to other observations. The oxidation state of C-2 is the same as that of carbon in isonitriles. The latter have a marked effect in stabilizing a lower oxidation state when they replace a saturated ligand such as water. Even CN^-, in spite of carrying a negative charge, has the same effect in a case such as Ru(III)/Ru(II), where a change from high-spin to low-spin form as H_2O is replaced by CN^- does not complicate matters as it does in the Fe(III)/Fe(II) case. Imidazole, when it is N-bound, does not appear to be a strong π acid. In the light of these considerations, it is in fact surprising that the effect of the C-bound compared to that of N-bound imidazole is not even greater than it is observed to be.

Attention has already been drawn to the sensitivity of E_f for the Ru(III)/Ru(II) couple to substitution on the imidazole, and the observation is repeated here simply in the interest of drawing together the various observations that require explanation.

The kinetics of substitution of NCS^- on $Ru(Me_2Im\text{-}C)^{3+}$ are peculiar enough so that we need to be certain that substitution was in fact being observed. We believe this to be the case because the electrochemical behavior of the species prepared from $Ru(Me_2Im\text{-}C)^{3+}$ and NCS^- is the same as that when $Ru(Me_2Im\text{-}C)(NCS)^+$ is first prepared and then oxidized. Just why outer-sphere association should be significant even in the second stage of binding to Ru(III) at concentrations of the order of 0.3 M NCS^- is not understood. According to our data, the inner-sphere isocyanate complex is rather robust. The rate of formation, 1.9×10^{-1} M^{-1} s^{-1}, combined with the equilibrium quotient leads to 0.6×10^{-5} s^{-1} for the rate of aquation.

The rearrangement of C-bound imidazole on Ru(II) to the N-bound form has not been observed, and since the reaction in the other direction does occur, we conclude that under our conditions the C-bound forms are more stable than the N-bound. Our experiments show that the carbon-bound isomer does not form to a significant extent directly from $Ru(NH_3)_5H_2O^{2+}$ and imidazole and is readily reached only through the N-bound form as an intermediate by an intramolecular process.

Reference to Table III shows that there are drastic differences in the yield of isomerized product depending on the substituents on imidazole, the yield being particularly low for the 1-methyl-substituted derivative (*N*-MeIm). The low yield in this case can be ascribed to ammine–methyl steric interference as can the high yield of $Ru(Me_2Im\text{-}C)^{2+}$. The polyfunctional nature of histidine may account for the fact that the yield of isomerized product is especially high for it.

Both isomerization and aquation are assisted by protons, but the protons may occupy different sites in the activated complexes for the two reactions. It is expected that the release of a proton from the 2-carbon, which may be a necessary prelude to rearrangement, almost certainly requires, first, that a free proton attack the ligand. For the proton-assisted aquation of NH_3, it has been suggested that the proton attacks the πd electrons of the metal. Such a path probably contributes in the case of imidazole, but because of the high rate of aquation in this case, and because the ligand has an exposed electron pair, it is likely that attack on the ligand also takes place.

Turning now to the data on substitution on $Ru(Me_2Im\text{-}C)^{2+}$, we note that, even when the charged ligands SCN^- and $Mepz^+$ are excluded, the rates of substitution span a large range, from $\sim 10^3$ M^{-1} s^{-1} in the case of H_2O_2 to <11 M^{-1} s^{-1} in the case of Im. This spread in rates contrasts sharply with the situation when $Ru(NH_3)_5H_2O^{2+}$ is reactant but is in harmony with trends observed for other trans-labilizing groups.[32] In fact, the sensitivity of rates to the nature of the incoming group may be general whenever the coordination sphere contains a π-acid ligand and may prove to be more pronounced for a more orthodox π acid such as NO^+ than it is for π acids that are also trans labilizing.

The comments just made imply that there is a real distinction between a class of orthodox ligands such as were featured in an article by Isied and Taube,[20] which include both saturated and strong π-acid ligands, and a class that has been referred to as being specifically trans labilizing. An orthodox π acid such as isn replacing NH_3 delabilizes in both the cis and the trans positions on Ru(II), and that is the case for a number of other π-acid ligands considered by Isied and Taube. By contrast, SO_3^{2-} in replacing NH_3 was shown to labilize Ru(II) trans, but delabilize cis. (It is not known however whether this property extends to other members of the specifically trans-labilizing class.) While SO_3^{2-}, C-bound imidazole, and other like ligands labilize both Ru(II) and Ru(III), the latter in fact more strongly than the former, there is no evidence that isn labilizes Ru(III). It is not to be expected that the distinction is sharp, but the consideration of the existing data on substitution suggests that it is meaningful.

In Figure 5, the data on the rates of substitution by isn on Ru(II), as affected by an auxiliary ligand, are shown plotted against E_f for the Ru(III)/Ru(II) couple. A plot of this kind was made by Isied et al.[20] and many of their data appear in Figure 5 clustering about the lower line. The surprising result is that the so-called trans-labilizing ligands appear to constitute a separate group, and the rates of substitution within that group also follow a correlation with E_f. Such a result is less surprising if there are different mechanisms for substitution in the two classes. A possibility is that in one group, e.g., that represented by the points clustering about the lower line, an intermediate is formed that has the shape of a square pyramid, while in the other class, a trigonal-bipyramidal intermediate (or activated complex) is formed. Unless the reactions for the more labile class are strongly S_N2 in character, a correlation of rate with E_f is also expected for it, an increased value of E_f implying a reduced electron density in the metal center and thus a lower rate of water release from the coordination sphere. For there to be a monotonic relation between E_f and k in each

---

[32] Scott, N. S.; Taube, H. *Inorg. Chem.* **1981**, *20*, 3135.

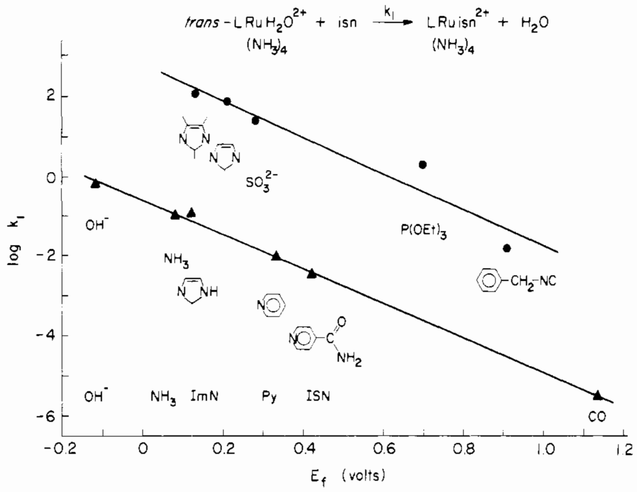

Figure 5. Effects of auxiliary ligands on the substitution lability of H_2O in ruthenium(II) ammines. Points identified by triangles are from Isied and Taube.[20] Circles identify data for ligands that are specifically trans labilizing: reproduced from ref 30 with permission of Gordon & Breach.

class, it is only required that there is a monotonic change in σ-donating capacity of the ligands as the π-acid character changes in the series.

Kristine[33] et al. have measured the specific rates for the reactions of $Ru(NH_3)_6^{2+}$ and of $Ru(NH_3)_5H_2O^{2+}$ with H_2O_2 at 25.2 °C as 2.1 and 1.8×10^2 M^{-1} s^{-1}. Substitution using a normal coordination position is not in question for the former but is a possibility for the latter. However, the specific rate of reaction is so much greater than that of substitution for any other neutral ligand (0.05–0.3 M^{-1} s^{-1} is usual)[16] that it seems unlikely that substitution is involved. The reaction of H_2O_2 with $Ru(Me_2Im\text{-}C)^{2+}$ is considerably more rapid than that with $Ru(NH_3)_5H_2O^{2+}$ in spite of the less favorable driving force, and in view of the much greater substitution lability of the former complex, we believe that the reaction of H_2O_2 with it does involve substitution.

Other important aspects of the reaction are left unsettled by our work, including the basic issue of whether the intermediate produced on the encounter of Ru(II) with H_2O_2 is HO or Ru(IV). We favor the latter on the basis that I^-, which is known to react rapidly with OH to form the relatively unreactive I or I_2^-, has no effect in improving the yield of $Ru(Me_2Im\text{-}C)^{3+}$. Our view makes it obligatory to assume that the Ru(IV) species reacts more rapidly by oxidizing the associated ligand than it does by oxidizing I^-.

One important issue in the reaction of O_2 with $Ru(Im\text{-}C)^{2+}$ appears to have been settled by our work, namely, that the reaction involves replacement of the labile water molecule by O_2. This conclusion follows from the observation that, when this position is preempted by NCS^-, the rate of reaction declines despite the fact that the thiocyanato complex is more strongly reducing than the aquo (E_f = 0.130 and 0.210, respectively). For any possible application of a ruthenium complex as a catalyst for the oxygen electrode, an inner-sphere mechanism may be mandatory if the high-energy intermediate O_2^- is to be avoided.[28] But it is to be noted that the turnover number for $Ru(Im\text{-}C)^{2+}$ in reaction with O_2 at atmospheric pressure is only 0.3 equiv s^{-1}. This species among those we have studied undergoes substitution most readily, yet the turnover number is still very low. Moreover, the reduction potential is well below the range in which any practical catalyst for the O_2 electrode must operate. Raising the potential simply by replacing ammonia with π acids will lead to a reduction in the turnover number. If a high turnover number and a high reduction potential are to be realized in a single complex, some new effects, which have not yet been exploited, will need to be introduced.

We are not at all certain of the nature of the product that is formed when $Ru(Im\text{-}C)^{2+}$ reacts with O_2 in excess. A proposal that is consistent with the observations is the following (or better, species in which some of the NH_3 shown is replaced by OH^-):

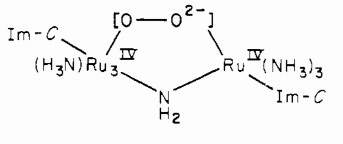

This would explain why excess O_2 is necessary (note that $O_2 + 2Ru^{II} \equiv [O_2]^{2-} + 2Ru^{III}$). The reduction with Eu^{2+} can be understood on the basis that Eu^{2+} reduces Ru(IV) to Ru(II) and O_2^{2-} to H_2O; ferrous ion as a weaker reducing agent only carries the reduction to the stage

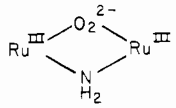

Reduction of the μ-peroxide coordinated to Co(III) is known to be a very slow process, and it is not surprising that the reaction with Fe^{2+}(aq) does not proceed beyond the stage indicated. The μ-NH_2 linkage explains why there is a proton titratable at a pH of 10.2 and the fact that at the Ru(III) stage of reduction the spectrum does not exactly match that of $Ru(Im\text{-}C)^{3+}$; reduction of the species proposed to be the 2+ stage would produce equal quantities of tetraammine and triammine, which should absorb similarly in the UV. The identification of the species RuP-275 is clearly worthy of further effort.

Acknowledgment. For most of the period during which the research reported here was done, M.F.T. was supported by an NIH postdoctoral Fellowship. This support is gratefully acknowledged, as is that by NIH Grant No. GM-13638 and NSF Grant No. CHE77-22722.

Registry No. $[(NH_3)_5Ru(Im\text{-}N)]Cl_3$, 51982-73-1; $[(NH_3)_5Ru(Me_2Im\text{-}N)]Cl_3$, 51982-74-2; $[(NH_3)_5Ru(Hist\text{-}N)]Cl_3$, 81873-37-2; $[(NH_3)_5Ru(BzIm\text{-}N)]Cl_3$, 51997-14-9; *trans*-$[(NH_3)_4ClRu(Im\text{-}C)]Cl_2$, 38118-33-1; *trans*-$[(NH_3)_4ClRu(Me_2Im\text{-}C)]Cl_2$, 38959-98-7; *trans*-$[(NH_3)_4ClRu(BzIm\text{-}C)]Cl$, 38959-99-8; $[(NH_3)_3Cl_2Ru(Me_2Im\text{-}C)]Cl$, 81802-37-1; $Ru(Me_2Im\text{-}C)^{3+}$, 81814-90-6; $[(NH_3)_5Ru(Im\text{-}C)]^{3+}$, 81802-38-2; $Ru(Me_2Im\text{-}N)^{2+}$, 81802-39-3; $Ru(N\text{-}MeIm\text{-}N)^{2+}$, 83697-79-7; $(NH_3)_5RuH_2O^{2+}$, 21393-88-4; $Ru(Im\text{-}N)^{2+}$, 39003-94-6; $Ru(Hist\text{-}N)^{2+}$, 81845-34-3; $Ru(BzIm\text{-}N)^{3+}$, 81802-40-6; $Ru(Im\text{-}C)^{2+}$, 60153-98-2; $Ru(Im\text{-}C)^{3+}$, 81802-41-7; $Ru(BzIm\text{-}C)^{2+}$, 81802-42-8; $Ru(BzIm\text{-}C)^{3+}$, 81802-43-9; $Ru(Me_2Im\text{-}C)(isn)^{2+}$, 60168-78-7; $Ru(Me_2Im\text{-}C)(isn)^{3+}$, 81802-44-0; $Ru(Me_2Im\text{-}C)(NCS)^+$, 81802-45-1; $Ru(Me_2Im\text{-}C)(NCS)^{2+}$, 81802-46-2; $Ru(Im\text{-}C)(NCS)^+$, 81814-91-7; $Ru(Im\text{-}C)(NCS)^{2+}$, 81814-92-8; *trans*-$[(H_2O)(NH_3)_4Ru(Im\text{-}N)]^{2+}$, 60251-41-4; *trans*-$[(H_2O)(NH_3)_4Ru(Im\text{-}N)]^{3+}$, 81802-47-3; *trans*-$[(OH)(NH_3)_4Ru(Me_2Im\text{-}C)]^{2+}$, 81802-48-4; *trans*-$[(Br)(NH_3)_4Ru(Me_2Im\text{-}C)]^{2+}$, 81802-49-5; *trans*-$[(Im\text{-}N)(NH_3)_4Ru(Me_2Im\text{-}C)]^{2+}$, 81802-50-8; *trans*-$[(Mepyr)(NH_3)_4Ru(Me_2Im\text{-}C)]^{3+}$, 81802-51-9; *trans*-$[(OH)(NH_3)_4Ru(Im\text{-}C)]^{2+}$, 81814-93-9; *trans*-$[(NCpyH)(NH_3)_4Ru(Im\text{-}C)]^{3+}$, 81814-94-0; *trans*-$[(isn)(NH_3)_4Ru(Im\text{-}C)]^{2+}$, 60153-97-1; *trans*-$[(CO)(NH_3)_4Ru(Im\text{-}C)]^{2+}$, 81872-15-3; $[(NH_3)_5Ru(Im\text{-}C^-)]^{2+}$, 81802-52-0; *trans*-$[(H_2O)(NH_3)_4Ru(Hist\text{-}C)]^{2+}$, 81802-53-1; *trans*-$[(H_2O)(NH_3)_4Ru(Hist\text{-}C)]^{3+}$, 81802-54-2; $[(NH_3)_5Ru(N\text{-}MeIm\text{-}N)]^{3+}$, 81802-55-3; $[(NH_3)_5Ru(H_2O)]^{2+}$, 21393-88-4; $[(NH_3)_5Ru(NCpyH)]^{3+}$, 81802-56-4; NCS^-, 302-04-5; Hist, 71-00-1; isn, 1453-82-3; $Mepyr^+$, 17066-96-5; H_2O_2, 7722-84-4; O_2, 7782-44-7.

---

[33] Kristine, F. J.; Johnson, C. R.; Donnell, S. O.; Shepherd, R. E. *Inorg. Chem.* **1980**, *19*, 2280.

[34] Skoog, D. A.; West, D. M. "Fundamentals of Analytical Chemistry", 2nd ed.; Holt, Rinehart and Winston: New York, 1969; p 680.